Chinese Journal of Natural Medicines

Inonotus obliquus (Chaga) against HFD/STZ-induced glucolipid metabolism disorders and abnormal renal functions by regulating NOS-cGMP-PDE5 signaling pathway

Yating FENG, Jing LIU, Le GONG, Zhaodi HAN, Yan ZHANG, Rongshan LI, Hui LIAO

Citation: Yating FENG, Jing LIU, Le GONG, Zhaodi HAN, Yan ZHANG, Rongshan LI, Hui LIAO, *Inonotus obliquus* (Chaga) against HFD/STZ-induced glucolipid metabolism disorders and abnormal renal functions by regulating NOS-cGMP-PDE5 signaling pathway, Chinese Journal of Natural Medicines, 2024, 22(7), 619-631. doi: 10.1016/S1875-5364(24)60616-3.

View online: https://doi.org/10.1016/S1875-5364(24)60616-3

Available online at www.sciencedirect.com
ScienceDirect
Chinese Journal of Natural Medicines 2024, **22**(7): 619-631
doi: 10.1016/S1875-5364(24)60616-3
Chinese Journal of Natural Medicines

•Original article•

Inonotus obliquus (Chaga) against HFD/STZ-induced glucolipid metabolism disorders and abnormal renal functions by regulating NOS-cGMP-PDE5 signaling pathway

FENG Yating[1], LIU Jing[1], GONG Le[1], HAN Zhaodi[2], ZHANG Yan[3], LI Rongshan[3], LIAO Hui[2*]

[1] *School of Pharmacy, Shanxi Medical University, Taiyuan 030001, China;*
[2] *Drug Clinical Trial Institution, The Fifth Hospital of Shanxi Medical University (Shanxi Provincial People's Hospital), Taiyuan 030012, China;*
[3] *Department of Nephrology, The Fifth Hospital of Shanxi Medical University (Shanxi Provincial People's Hospital), Taiyuan 030012, China*

Available online 20 Jul., 2024

[ABSTRACT] Our prior investigations have established that *Inonotus obliquus* (Chaga) possesses hypoglycemic effects. Persistent hyperglycemia is known to precipitate renal function abnormalities. The functionality of the kidneys is intricately linked to the levels of cyclic guanosine-3',5'-monophosphate (cGMP), which are influenced by the activities of nitric oxide synthase (NOS) and phosphodiesterase (PDE). Enhanced cGMP levels can be achieved either through the upregulation of NOS activity or the downregulation of PDE activity. The objective of the current study is to elucidate the effects of Chaga on disorders of glucolipid metabolism and renal abnormalities in rats with type 2 diabetes mellitus (T2DM), while concurrently examining the NOS-cGMP-PDE5 signaling pathway. A model of T2DM was developed in rats using a high-fat diet (HFD) combined with streptozotocin (STZ) administration, followed by treatment with Chaga extracts at doses of 50 and 100 $mg \cdot kg^{-1}$ for eight weeks. The findings revealed that Chaga not only mitigated metabolic dysfunctions, evidenced by improvements in fasting blood glucose, total cholesterol, triglycerides, and insulin resistance, but also ameliorated renal function markers, including serum creatinine, urine creatinine (UCr), blood urea nitrogen, 24-h urinary protein, and estimated creatinine clearance. Additionally, enhancements in glomerular volume, GBM thickness, podocyte foot process width (FPW), and the mRNA and protein expressions of podocyte markers, such as nephrin and wilms tumor-1, were observed. Chaga was found to elevate cGMP levels in both serum and kidney tissues by increasing mRNA and protein expressions of renal endothelial NOS and neural NOS, while simultaneously reducing the expressions of renal inducible NOS and PDE5. In summary, Chaga counteracts HFD/STZ-induced glucolipid metabolism and renal function disturbances by modulating the NOS-cGMP-PDE5 signaling pathway. This research supports the potential application of Chaga in the clinical prevention and treatment of T2DM and diabetic nephropathy (DN), with cGMP serving as a potential therapeutic target.

[KEY WORDS] *Inonotus obliquus*; Diabetic nephropathy; Glucolipid metabolism disorders; Renal functions; NOS-cGMP-PDE5 signaling

[CLC Number] R965 **[Document code]** A **[Article ID]** 2095-6975(2024)07-0619-13

Introduction

Inonotus obliquus (Fr.) Pilat (Chaga), a member of the Hymenochaetaceae family, is recognized for its nutritional value and traditional medicinal use in Russia, China and Japan. Chaga is known for its anticancer, antiviral, immunemodulating, and hypoglycemic effects [1]. A particular study demonstrated that Chaga mitigates insulin resistance and lipid metabolism dysfunctions in diabetic mice through the PI3K/Akt and AMPK/ACC signaling pathways [2]. Our latest research revealed that Chaga decreases blood glucose levels and proteinuria in diabetic nephropathy (DN) rats induced by a high-fat diet (HFD) and streptozotocin (STZ) [3].

Diabetes mellitus (DM) is defined by chronically elevated blood glucose levels, along with associated metabolic disorders such as obesity, hyperlipidemia, and abnormal in-

[Received on] 04-Jan.-2024
[Research funding] This work was supported by the Medical Key Research Projects of Shanxi Province (No. 2020XM02), the Local Science and Technology Development Funds Projects Guided by Central Government (No. YDZJSX2021C027), the Basic Research Program of Shanxi Province (No. 202103021224370), the Key R & D Project of Shanxi Province [International Scientific and Technological Cooperation, Independent Topics, (No. 201903D421061)], and Wu Jieping Medical Foundation (No. 320.6750.2021-08-10).
[*Corresponding author] E-mail: huiliao@263.net
These authors have no conflict of interest to declare.

sulin resistance [4]. The International Diabetes Federation reports a 1.62-fold increase in the number of adults diagnosed with diabetes, reaching 463 million in 2019 compared to 2009, with 95% of these cases being type 2 diabetes mellitus (T2DM) [5]. DN stands as one of the most severe complications of T2DM, with approximately 30% to 40% of patients with T2DM patients developing diabetic kidney injury. DN is primarily diagnosed through the presence of proteinuria and diminished renal function, marked by changes in serum creatinine (SCr), blood urea nitrogen (BUN), 24-h urinary protein (24h-UP) levels, and the estimated glomerular filtration rate (eGFR) [6]. Proteinuria, indicative of podocyte damage, is a critical clinical sign of DN. Podocytes, which form an essential part of the glomerular filtration membrane, are terminally differentiated, structurally distinctive, and highly specialized cells crucial for maintaining kidney function [7].

The cyclic guanosine-3',5'-monophosphate (cGMP) signaling cascade plays a pivotal role in regulating various renal functions. Disruptions in cGMP signaling are linked to increased renal damage and podocyte lesions, whereas enhancements in cGMP-dependent pathways have been shown to improve renal and podocyte function [8]. Elevated glucose levels lead to a reduction in cGMP within podocytes, conversely, increasing cGMP levels can enhance glucose uptake and decrease the permeability of the albumin filtration barrier [9]. Inorganic dietary nitrate has been found to mitigate obesity induced by HFD and to rectify disturbed glucolipid metabolism through the nitric oxide (NO)-cGMP pathway [10]. The regulation of cGMP levels involves activities of three isoforms of nitric oxide synthase (NOS) and phosphodiesterase (PDE) [11]. Emerging evidence indicates that inhibitors of phosphodiesterase 5 (PDE5i) may offer significant renal protective effects [12].

This study focuses on exploring the impact of the NOS-cGMP-PDE5 pathway modulation by Chaga on improving disorder in glucose and lipid metabolism as well as renal functions. To this end, after the establishment of a T2DM rat model, we monitored serum cGMP levels across different stages: the pre-T2DM stage (characterized by metabolic disorders), the T2DM stage (defined by persistent hyperglycemia and metabolic disorders), and the DN stage (marked by abnormal SCr, BUN, and proteinuria) in T2DM-induced DN rats. Additionally, cGMP levels in the kidney tissues, eNOS, iNOS, nNOS and PDE5, were comprehensively investigated. The aim of this research is to elucidate the effects and potential mechanisms of Chaga on glucolipid metabolism disorders during the T2DM stage and renal injury in the DN stage, thereby providing a sound basis for Chaga's clinical application.

Material and Methods

Materials

Chaga, collected from the Lvliang Mountains in Shanxi Province, was authenticated as *Inonotus obliquus* by Prof. GUO Shang at the Shanxi Institute for Functional Food, Shanxi Agricultural University (Taiyuan, China). Chaga extracts with 13.7% polysaccharide and 1.9% polyphenols, generously provided by Professor GUO, were utilized. The polysaccharide content was determined using the phenol-sulfuric acid method [11], and the polyphenol content was assessed by the Folin-Ciocalteu method [13]. The diets for the study, both a standard chow and a HFD, were sourced from Boaigang Biotechnology Company (Beijing, China). The nutrient composition of the ordinary diet was 12.0% fat, 20.6% protein, and 67.4% carbohydrates by energy percentage. Conversely, the HFD composition was 35.5% fat, 20.6% protein, and 43.9% carbohydrates. The STZ used in the study was procured from Sigma (USA).

Animal experiments

Male Sprague–Dawley rats, aged 5 weeks and weighing 124.6 ± 12.3 g, were acquired from the Laboratory Animal Center at the Shanxi Provincial People's Hospital [Taiyuan, China; experimental animal production license No. SCXK (Jin) 2019-0001]. The conduct of all animal experiments was in strict adherence to national guidelines and relevant laws for animal protection. Furthermore, the experimental procedures involving animals were approved by the Ethical Committee for the Experimental Use of Animals at Shanxi Provincial People's Hospital (approval No. 2021-305), ensuring compliance with ethical standards. The rats were accommodated under specific pathogen-free conditions with an air-conditioning system maintaining a temperature of 24 ± 2 °C and a humidity of 50% ± 5%, alongside a 12-h light/dark cycle [laboratory animal environment certificate No. SYXK (Jin) 2019-0003]. They had unrestricted access to both food and water. Following a week of acclimatization on a standard diet, the rats were categorized randomly into four groups, each consisting of six rats: a NOR group, a DN model group, a low-dose Chaga treatment group (DN + I), and a high-dose Chaga treatment group (DN + II). The NOR group rats were maintained on a standard diet for the entire 17 weeks of the study. To induce DN, rats were fed a HFD for 8 weeks. Upon confirmation of metabolic disorder, rats designated for the DN model were administered a single intraperitoneal injection of 35 $mg \cdot kg^{-1}$ STZ and continued on the HFD for an additional eight weeks. Simultaneously, the treatment groups received Chaga extracts *via* oral gavage at doses of 50 and 100 $mg \cdot kg^{-1}$, respectively, alongside their HFD regimen, administered daily for eight weeks.

Body weight (BW) was systematically recorded on a weekly basis. Prior to STZ-induction, blood samples were collected *via* the cardiac blood sampling method to confirm metabolic disorder, as part of the biochemistry assay [14]. Following the STZ injection, rats with random blood glucose (RBG) levels of ≥ 16.7 $mmol \cdot L^{-1}$ at both 3 [15] and 7 d [16] post-injection were classified as successful T2DM models. At the study's conclusion in the 17th week, all animals were euthanized under anesthesia, and serum and kidney tissues were harvested for biochemistry assays and pathological analysis, respectively. This experimental design is depicted in Fig. 1.

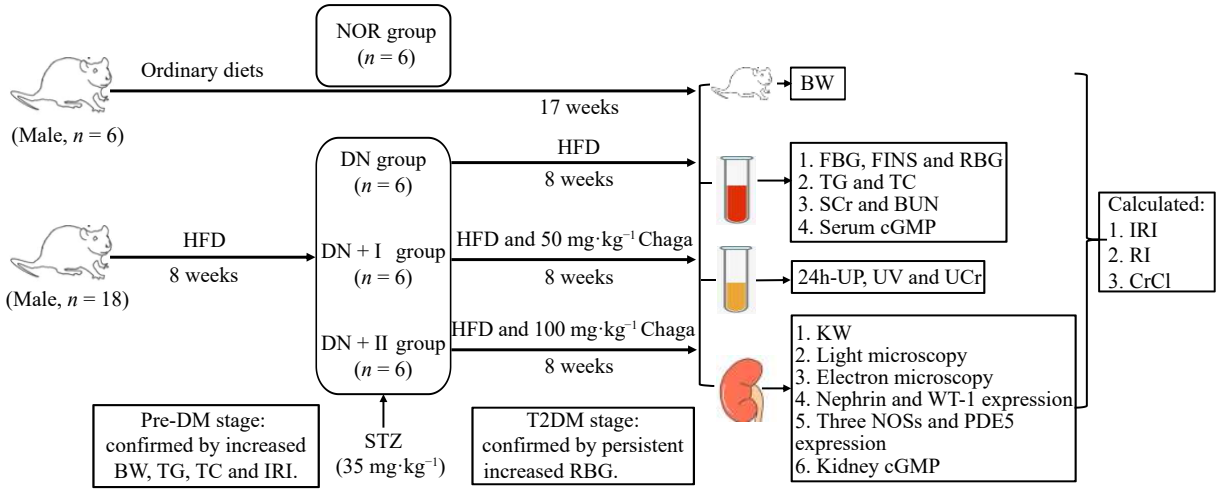

Fig. 1 Schematic diagram of HFD/STZ-induced T2DM and Chaga intervention on rats. BUN: blood urea nitrogen; BW: body weight; cGMP: cyclic guanosine-3',5'-monophosphate; CrCl: creatinine clearance; DN, diabetic nephropathy; DN + I, DN rats treated with 50 mg·kg^{-1} Chaga extracts per day; DN + II: DN rats treated with 100 mg·kg^{-1} Chaga extracts per day; FBG: fast blood glucose; FINS: fast insulin; HFD: high fat diet; IRI, insulin resistance index; KW: kidney weight; NOR: normal control; NOS: nitric oxide synthases; PDE5: phosphodiesterase 5; RBG: random blood glucose; SCr: serum creatinine; STZ: streptozotocin; T2DM: type 2 diabetes mellitus; TC: total cholesterol; TG: triglyceride; 24h-UP: 24 h urinary protein; UCr: urine creatinine; UV: 24 h urine volume; WT-1: Wilms' tumor-1.

Glucolipid metabolism disorders evaluation

Obesity in rats was confirmed when their body weight (BW) was at least 20% higher than that of normal-weight rats, in accordance with established criteria [17].

To verify the presence of insulin resistance, the levels of fasting insulin (FINS) and fasting blood glucose (FBG) were measured. The insulin resistance index (IRI) was then calculated using the formula derived from the homeostatic model assessment of insulin resistance (HOMA-IR), as follows [18]:

$$\text{IRI} = \frac{\text{FBG (mmol}\cdot\text{L}^{-1}) \times \text{FINS (mIU}\cdot\text{L}^{-1})}{22.5} \quad (1)$$

The analyses of FINS and FBG were conducted using Roche ACCU-CHEK Performa devices (Roche Diabetes Care GmbH, Mannheim, Germany). Additionally, the levels of plasma triglycerides (TG) and total cholesterol (TC) were measured using AU5800 with ISE biochemistry analyzers (Beckman Coulter, Germany) to confirm hyperlipidemia.

Measurement of renal index

After euthanizing the rats at the conclusion of the 17th week, both the right and left kidneys were harvested and their combined weight (KW) was accurately measured using a JA3003 precision electronic balance, with an accuracy of 0.001 g. This process involved severing the blood vessels, excising connective tissue and fat, and removing any blood from the surface of the kidneys. The BW of each rat was also recorded at the end of the 17th week prior to euthanasia. The renal index (RI) for each rat was then calculated using the formula [19].

$$\text{RI} = \frac{\text{KW (mg)}}{\text{BW (g) at the 17}^{th}\text{ week}} \quad (2)$$

Renal function evaluation

To assess renal function accurately, each rat was housed in a metabolic cage for 24 h to facilitate the collection of urine. During this period, rats were deprived of food but had access to water. The volume of urine (UV) collected over 24 h was meticulously recorded, and the samples were subsequently stored at −80 °C for further analysis. The levels 24 h-UP and urine creatinine (UCr) levels were determined using commercial kits provided by Jiancheng Bioengineering Company (Nanjing, China). Additionally, the levels of SCr and BUN were measured using AU5800 ISE biochemistry analyzers (Beckman Coulter, Germany).

The estimated creatinine clearance (CrCl), serving as a proxy for the glomerular filtration rate and thus a measure of kidney function, was calculated for each rat using the following formula [20]:

$$\text{CrCl (mL}\cdot\text{min}^{-1}\cdot\text{kg}^{-1}) = \frac{\text{UCr (mmol}\cdot\text{L}^{-1}) \times \text{UV (mL)}}{\text{SCr (mmol}\cdot\text{L}^{-1}) \times 1440\text{ (min)} \times \text{BW (kg)}} \quad (3)$$

Pathological examination

Light microscopy

Freshly dissected kidneys were fixed in 10% neutral formalin buffer, embedded in paraffin. The embedded kidney was cut into 3 μm thick sections with Leica Microtome. The sections were stained with Periodic Acid-Schiff reagent, and the morphological changes of glomerulus were observed with KF-PRO-005-EX digital scanner (Motic, Xiamen, China).

The images were selected randomly in which the glomerulus number was no more than twenty and were analyzed with K-Viewer (1.5.3.1) image analysis software (× 400, KFMI, China). The length of the two longest perpendicular diameters in each glomerular capillary tuft without Bowman's space was measured in μm, and then the mean value was calculated from 10 images. The areas of the glomerular mes-

angial region and capillary tuft were measured. The relative area of the mesangial region (%) was calculated according to the formula [21].

$$\text{The relative area (\%)} = \frac{\text{Area of the mesangial region}}{\text{Area of the capillary tuft}} \times 100 \quad (4)$$

Electron microscopy

Freshly dissected kidneys were fixed using 2.5% glutaraldehyde. The ultrathin sections were stained with uranium acetate-lead citrate for electron microscopy. For each specimen, ten photographs (× 20 000 magnification) covering different regions in the glomerular cross section were taken separately.

The thickness of glomerular basement membrane (GBM), the length of the peripheral GBM and the number of slit pores were all measured. Images were selected and analyzed using the RADIUS Control & Imaging software (EMSIS ASIA, Germany). The mean of the foot process width (FPW) was calculated as follows [21].

$$\text{FPW} = \frac{\pi}{4} \times \frac{\sum \text{GBM length}}{\sum \text{slits}} \quad (5)$$

where ∑slits are the total number of slits counted and ∑GBM length is the total GBM length measured in one glomerulus.

ELISA analysis

For the enzyme-linked immunosorbent assay (ELISA) analysis conducted at the conclusion of the 17th week, the concentrations of cyclic guanosine-3',5'-monophosphate (cGMP) in both serum and renal tissue homogenates (prepared at a concentration of 100 mg tissue/mL homogenate) were determined. To perform these measurements, ELISA kits (Lot No. MM-0027R1, Meimian, Jiangsu, China) were utilized. All samples, alongside controls, were assayed in sextuplicate to ensure the accuracy and reliability of the results obtained.

Quantitative real-time PCR analysis

Thirty milligrams of renal cortical tissue were meticulously dissected and immediately placed on ice before being finely minced. The expression levels of nephrin, Wilms' tumor-1 (WT-1), eNOS, nNOS, inducible iNOS, and PDE5 mRNAs were quantitatively analyzed *via* real-time polymerase chain reaction (RT-PCR). Total RNA was extracted using the Trizol reagent, with subsequent assessment of RNA concentration and purity to ensure optimal sample quality. Quantitative RT-PCR analyses were conducted employing the 2X M5 HiPer SYBR Premix EsTaq (Mei5 Biotechnology, Co., Ltd.) on a CFX96 Real-Time System (Bio-Rad Laboratories, Inc.). The glyceraldehyde 3-phosphate dehydrogenase (GAPDH) gene served as an internal reference to normalize the expression data. Relative quantification of gene expression was calculated utilizing the $2^{-\Delta\Delta Ct}$ method, thereby facilitating accurate comparisons of mRNA levels across different samples.

Western blotting

Thirty milligrams of rat kidney cortical tissue were meticulously prepared on ice, cut into small pieces. For the extraction of proteins, RIPA lysis buffer (Solarbio Science & Technology, Beijing, China), enriched with 1% protease inhibitor, was applied at a ratio of 1 ∶ 10 (mg ∶ μL). The tissues underwent mechanical homogenization followed by ultrasonication for 30 s on ice to ensure thorough disruption. Subsequent to a 30-min lysis on ice, the homogenate was centrifuged at 4 °C for 20 min at 12 000 r·min^{-1}. The concentration of proteins in the supernatant was quantified using commercial assay kits (Meimian Industrial Company, Jiangsu, China).

For protein analysis, samples containing 50 μg of protein were subjected to sodium dodecyl sulfate–polyacrylamide gel electrophoresis (SDS-PAGE) and subsequently transferred onto polyvinylidene fluoride (PVDF) membranes. These membranes were blocked with nonfat dried milk for 2 h to prevent nonspecific binding, followed by incubation with primary antibodies: eNOS (catalog No. 20116-1-AP, Proteintech, Wuhan, China), iNOS (catalog No. 18985-1-AP, Proteintech, Wuhan, China), and WT-1 (catalog No. 12609-1-AP, Proteintech, Wuhan, China) at a 1 ∶ 1000 dilution; nNOS (catalog No. bs-0156R, Bioss, Beijing, China) and PDE5 (catalog No. bs-2349R, Bioss, Beijing, China) at a 1 ∶ 500 dilution; and nephrin (catalog No. Ab216341, Abcam, USA) at a 1 ∶ 2000 dilution, all incubated at 4 °C. Following this,

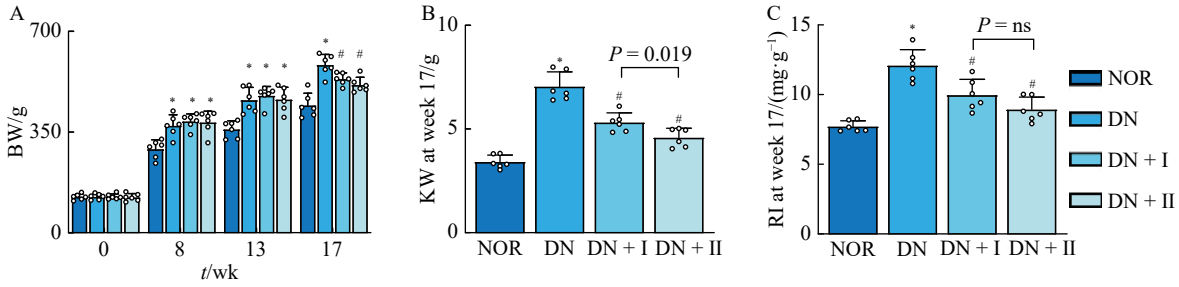

Fig. 2 Effects of Chaga on obesity and kidney coefficients. (A) Weighing of BW by electronic balance. (B) Weighing of KW by electronic balance. (C) Calculation of RI according to equation (2). NOR: normal control; DN: diabetic nephropathy; DN + I: DN rats treated with 50 mg·kg^{-1}·d^{-1} Chaga extracts; DN + II: DN rats treated with 100 mg·kg^{-1}·d^{-1} Chaga extracts; BW: body weight; KW: kidney weight; RI: renal index. Data were presented as mean ± SD (n =6). $^{*}P$ < 0.05 *vs* the NOR group at the same week; $^{\#}P$ < 0.05 *vs* the DN group at the same week.

membranes were washed four times (15 min each) and then incubated with corresponding secondary immunoglobulin G (IgG) conjugated to horseradish peroxidase (HRP) antibody (catalog No. SA00001-2, Proteintech, Wuhan, China) at room temperature for 1 h. Detection and quantitative analysis of the protein bands were performed using the Quantity One analysis system (Bio-Rad, Hercules, CA, USA). GAPDH (catalog No. 10494-1-AP, Proteintech, Wuhan, China) served as the internal loading control, used at a dilution of 1 ∶ 5000.

Statistical analysis

Statistical analyses were performed using SPSS 23.0 software (IBM, NY, USA). Data are presented as mean ± standard deviation (SD). Differences between two groups were assessed using Student's *t*-test. All *P* values reported are two-tailed, with a *P* value of less than 0.05 deemed to indicate statistical significance.

Results

Chaga improved obesity and kidney coefficients

To investigate whether Chaga mitigates obesity and kidney abnormalities induced by a HFD/STZ, we monitored BW, KW, and RI of rats (Fig. 2).

BW of changes for each group at the 0, 8th, 13th, and 17th weeks are illustrated in Fig. 2A. Initially, at week 0, there were no significant differences in BW between the DN and NOR groups (*P* = not significant). However, at the 8th, 13th, and 17th weeks, the BW of the DN group was significantly higher than that of the NOR group (all: $P < 0.01$), with increases of 26.5%, 25.7%, and 26.2%, respectively, categorizing the rats in the DN group as obese [17]. By the 17th week, the weights of both DN + I and DN + II groups were significantly reduced compared to the DN group ($P < 0.05$ for both), indicating that Chaga could counteract HFD/STZ-induced obesity.

Figs. 2B and 2C present the kidney weight and renal index, respectively. The KW of the DN group was significantly higher than those of the NOR group ($P < 0.01$), while the KWs of the DN + I and DN + II groups were significantly lower than those of the DN group ($P = 0.001$ and $P < 0.001$, respectively), with the decrease in the DN + II group being more pronounced than in the DN + I group ($P = 0.019$). Similarly, the RI was significantly higher in the DN group compared to the NOR group ($P < 0.001$), but it was significantly lower in both the DN + I and DN + II groups compared to the DN group ($P < 0.01$ for both). These findings suggest that Chaga effectively improves kidney coefficients in the context of HFD/STZ-induced conditions.

Chaga improved HFD/STZ-induced glucolipid metabolism disorders

To verify Chaga's impact on HFD/STZ-induced glucolipid metabolism disorders, we measured FBG, FINS and IRI of rats (Fig. 3).

FBG of each group at the 0 and 8th week were shown in Fig. 3A. At the 17th week, the DN group exhibited significantly elevated FBG levels compared not only to the NOR group but also relative to its 8th-week levels ($P < 0.001$ for both comparisons). The Chaga-treated groups showed significant reductions in FBG at the 17th week compared to the DN group ($P < 0.001$), with the DN + II group demonstrating a notably better effect ($P = 0.044$).

Figs. 3B and 3C display the FINS and IRI measurements. By the 8th week, increases in FINS and IRI of the DN, DN + I, and DN + II groups compared to the NOR group ($P < 0.05$ for all). By the 17th week, FINS in the DN group had signific-

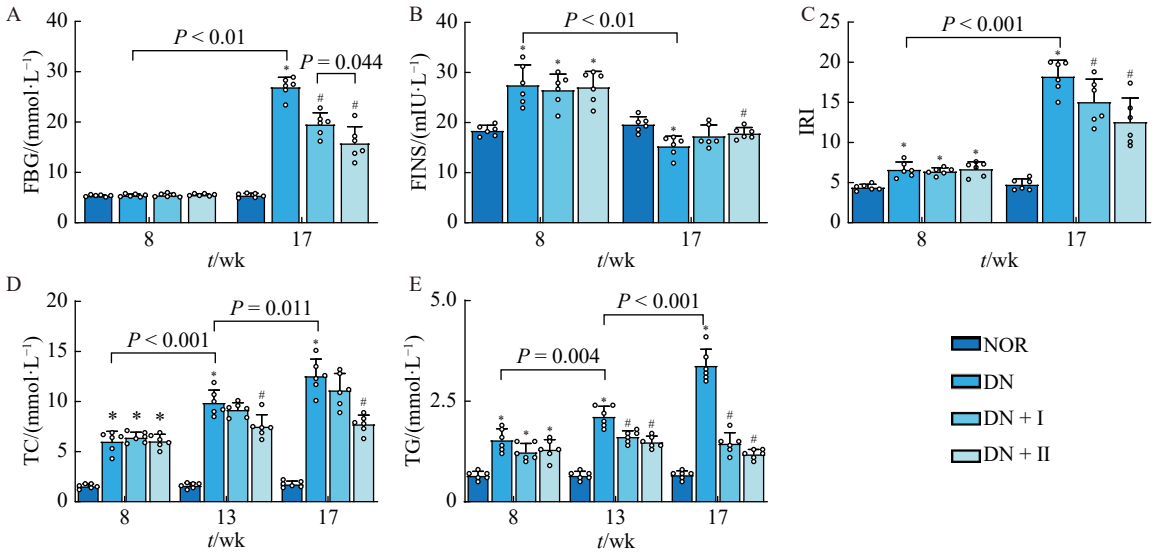

Fig. 3 Effects of Chaga on HFD/STZ-induced glucolipid metabolism disorders. (A) FBG: fasting blood glucose. (B) FINS: fasting insulin. (C) IRI: insulin resistance index. (D) TC: total cholesterol. (E) TG: triglyceride. NOR: normal control; DN: diabetic nephropathy; DN + I: DN rats treated with 50 mg·kg^{-1}·d^{-1} Chaga extracts; DN + II: DN rats treated with 100 mg·kg^{-1}·d^{-1} Chaga extracts. Data were presented as mean ± SD ($n = 6$). $^{*}P < 0.05$ *vs* the NOR group at the same week. $^{\#}P < 0.05$ *vs* the DN group at the same week.

antly reduced compared to both the NOR group at the same time point and its own 8th-week levels (P = 0.002 and P < 0.001, respectively), with the DN + II group showing a significant increase over the DN group (P = 0.021). IRI was significantly higher in the DN group compared to both the NOR group at the 17th week and its own 8th-week levels (P < 0.001), with significant reductions observed in the Chaga-treated groups compared to the DN group (P < 0.01).

In our study, no significant changes were observed in the RBG levels within the NOR group before and after administration of a buffer solution, indicating stability in their glucose levels (P = ns). Conversely, following 3 d and 7 d of post-STZ injection, the RBG levels in the DN, DN + I, and DN + II groups experienced significant increases compared to their pre-STZ injection levels (P < 0.001 for all), surpassing the critical threshold of 16.7 mmol·L^{-1} [15, 16], indicative of induced diabetes.

Regarding lipid metabolism, Figs. 3D and 3E display the total TC and TG levels in serum at the 8th, 13th, and 17th weeks. The DN group showed significantly elevated TC and TG levels at these time points compared to the NOR group (P < 0.05 for all instances). Notably, within the DN group, both TG and TC levels saw a significant increase at the 13th week relative to the 8th week (P < 0.01 for both), with a further significant rise from the 13th to the 17th week (P < 0.01 for both). When comparing the DN group to the Chaga-treated groups, the DN + I group exhibited lower TC and TG levels at the 13th and 17th weeks, though significant differences were observed only in TG levels (P < 0.05). The DN + II group demonstrated a significant reduction in both TC and TG levels at the 13th and 17th weeks (P < 0.05 for all), indicating a more pronounced effect of Chaga treatment on ameliorating glucolipid metabolism disorders induced by HFD/STZ.

Chaga ameliorated HFD/STZ-induced renal dysfunction

To experimentally ascertain whether Chaga could alleviate HFD/STZ-induced renal dysfunction, we conducted comprehensive measurements, including SCr, BUN, 24h-UP, UCr, and CrCl, alongside observations of glomerular morphology (Fig. 4).

The SCr, BUN, and 24h-UP levels of each group at 8th, 13th, and 17th weeks are shown in Figs. 4A–4C. By the 17th week, these levels in the DN group were significantly elevated compared to both the NOR group at the same time point and the DN group's own measurements at the 13th week (P < 0.05 for all comparisons). The end-of-experiment UCr and CrCl levels are presented in Figs. 4D and 4E. The DN group's UCr level was markedly lower than that of the NOR group (P < 0.001), and the DN group's CrCl (6.32 ± 0.96 mL·min^{-1}·kg^{-1}) was significantly reduced compared to the NOR group (10.13 ± 1.51 mL·min^{-1}·kg^{-1}, P = 0.015). Intervention with Chaga resulted in significant improvements in SCr, BUN, 24h-UP, and UCr compared with the DN group (P < 0.05 for all). Notably, a significant increase in CrCl was observed only in the DN + II group (P = 0.005), indicating Chaga's potential in improving renal filtration dysfunction induced by HFD/STZ.

Histopathological glomerulus staining images for the NOR, DN, DN + I, and DN + II groups are displayed in Fig. 4F. Relative to the NOR group, the DN group exhibited notable glomerular hypertrophy and expansion of the mesangial matrix. Chaga treatment significantly mitigated these pathological alterations [22]. The mean glomerular diameter in the DN group was significantly larger than that in the NOR group (P < 0.001). Moreover, compared to the NOR group, the relative mesangial area in the DN group was significantly increased (P < 0.001). Both DN + I and DN + II groups showed significant improvements in these renal pathological changes. These findings suggest that Chaga has the potential to ameliorate HFD/STZ-induced alterations in kidney function and histomorphology.

Chaga ameliorated HFD/STZ-induced renal podocytes injury

To substantiate that Chaga could mitigate renal podocyte injury induced by a HFD/STZ, we measured the mean GBM thickness, FPW, and the expression levels of podocyte markers nephrin and WT-1 in rats (Fig. 5).

Electron microscopic examinations of the GBM and foot processes of podocytes are presented in Fig. 5A, illustrating segmental fusion of podocyte foot processes: a hallmark of podocyte injury in the DN rats [23]. The red arrows highlight the foot processes, while the white arrows point to the GBM. The DN group exhibited a significantly increased mean GBM thickness compared to the NOR group (P < 0.001), with both Chaga intervention groups showing notably reduced thicknesses compared to the DN group. The reduction in GBM thickness was more pronounced in the DN + II group than in the DN + I group (P < 0.001). Similarly, FPW was significantly greater in the DN group compared to the NOR group (P < 0.001), with both Chaga-treated groups demonstrating significant reductions in FPW compared to the DN group (P = 0.001 and P < 0.001, respectively), indicating partial reversal of foot process fusion by Chaga intervention.

The mRNA and protein expressions of nephrin and WT-1, shown in Figs. 5B and 5C, were significantly lower in the DN group compared to the NOR group. Both the DN + I and DN + II groups exhibited significant increases in the expression levels of these podocyte markers compared to the DN group (all: P < 0.01). These findings indicate that the morphological and podocyte injuries induced by HFD/STZ were effectively reversed by Chaga treatment, highlighting its therapeutic potential in addressing renal podocyte damage.

Chaga reversed the HFD/STZ-induced decrease of cGMP levels in serum and kidney tissues

Analyzing the impact of Chaga on regulating glucolipid metabolism disorders and attenuating kidney damage, we assessed cGMP levels in both serum and kidney tissues of rats, illustrated in Fig. 6.

Fig. 6A reveals that the serum cGMP levels in the diabetic nephropathy (DN) group at both the 13th and 17th weeks were significantly reduced compared to their levels at the 8th week (P = 0.002 and P = 0.001). Furthermore, these levels at

the 13th and 17th weeks were notably lower than those in the normal control (NOR) group at the corresponding times ($P < 0.01$ for both). In contrast, Chaga treatment in the DN + I and DN + II groups significantly elevated serum cGMP levels at these time points when compared to the DN group ($P < 0.001$ for all).

Fig. 6B shows that while the kidney cGMP level in the DN group was lower than in the NOR group, this difference was not statistically significant (P = ns). However, Chaga treatment led to an increase in kidney cGMP levels, with a significant effect observed in the DN + II group compared to the DN group ($P < 0.05$). These findings demonstrate that the decrease in cGMP levels induced by HFD/STZ was effectively reversed by Chaga intervention.

Chaga increased renal eNOS, nNOS and decreased iNOS, PDE5 expression

To elucidate the mechanism through which Chaga enhances cGMP levels, we analyzed the expression of NOS and PDE5 in rat kidney tissues (Fig. 7).

Fig. 7A presents the mRNA expression levels of renal eNOS, nNOS, iNOS, and PDE5. It was observed that the expression level of eNOS was significantly reduced in the DN group compared to the NOR group ($P < 0.01$), whereas the expression levels of iNOS and PDE5 were significantly elevated in the DN group in comparison to the NOR group ($P < 0.01$ for both). The expression level of nNOS did not signific-

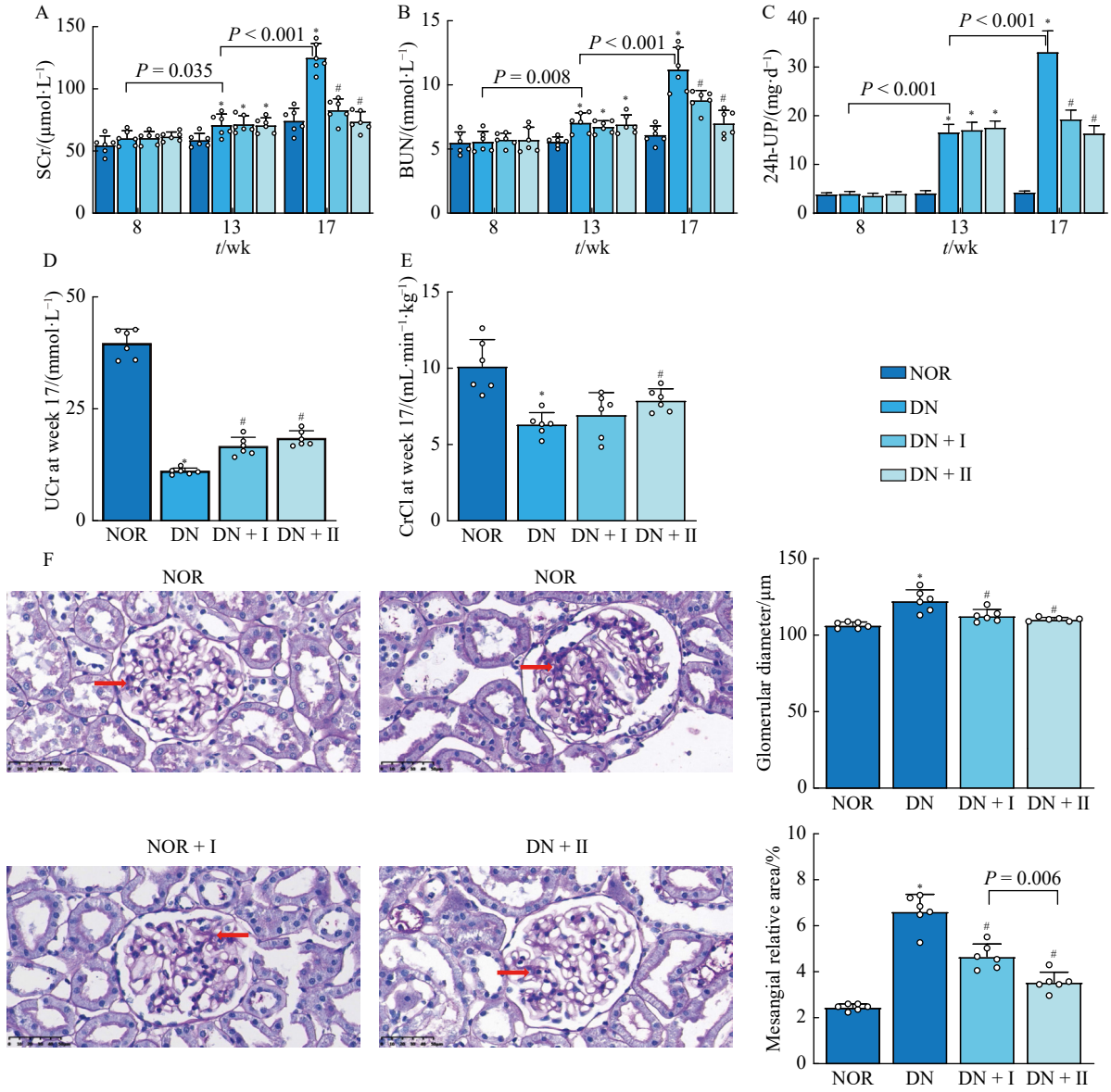

Fig. 4 Testing of kidney function indicators and histological examination of kidney tissue sections. (A) SCr: serum creatinine. (B) BUN: blood urea nitrogen. (C) 24h-UP: 24 h urinary protein. (D) UCr: urea creatinine. (E) CrCl: creatinine clearance. (F) Kidney tissue sections were stained with PAS (× 400). NOR: normal control; DN: diabetic nephropathy; DN + I: DN rats treated with 50 mg·kg^{-1}·d^{-1} Chaga; DN + II: DN rats treated with 100 mg·kg^{-1}·d^{-1} Chaga; Data were presented as mean ± SD (n = 6). $^{*}P < 0.05$ *vs* NOR; $^{\#}P < 0.05$ *vs* DN.

antly differ between the DN and NOR groups (P = ns).

Fig. 7B displays the protein expression levels of eNOS, nNOS, iNOS, and PDE5. Consistent with the mRNA findings, the protein expression levels of nNOS and eNOS in the DN group were significantly decreased, whereas those of iNOS and PDE5 were significantly increased compared to the NOR group ($P < 0.01$ for all comparisons).

In both Chaga-treated groups (DN + I and DN + II), mRNA, and protein expression levels of eNOS and nNOS were significantly increased, while those of iNOS and PDE5 were significantly decreased in comparison to the DN group ($P < 0.01$ for all). These results demonstrate that Chaga enhances cGMP levels primarily through the upregulation of eNOS and nNOS and the downregulation of iNOS and PDE5 expressions.

Discussion

Intervention strategies targeting blood glucose control and the amelioration of metabolic disorders have been established as effective measures for preventing DN [24]. In our study, we observed significant markers of metabolic disorder—including obesity, insulin resistance, and hyperlipidemia—alongside persistent hyperglycemia. These findings indicate that Chaga treatment yielded notable improvements in glucose and lipid metabolism disorders before the progression of T2DM to the DN stage. Although controlling hyperglycemia is a pivotal strategy for averting kidney injury, a substantial number of patients with T2DM eventually develop DN or even end-stage kidney disease [24]. Thus, exploring the renal protective effects of Chaga, while verifying its impact on glucose and lipid metabolism disorders, holds signi-

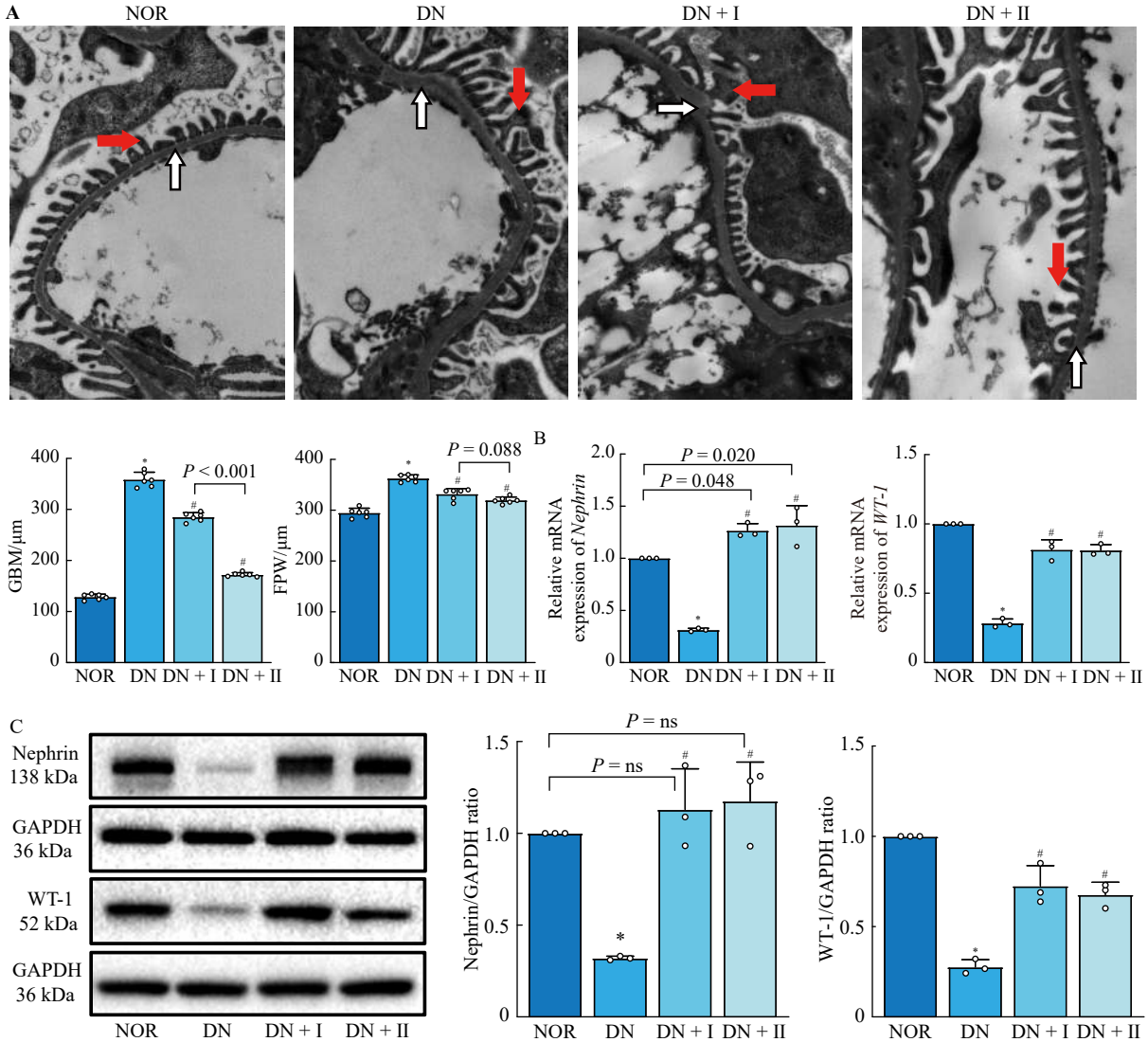

Fig. 5 Effects of Chaga on HFD/STZ-induced podocytes injury. (A) Observation of GBM and FPW by electron microscopy (× 20 000). (B) Expression of *Nephrin* and *WT-1* by RT-PCR. (C) Expression of Nephrin and WT-1 by Western blot. NOR: normal control; DN: diabetic nephropathy; DN + I: DN rats treated with 50 mg·kg^{-1}·d^{-1} Chaga; DN + II: DN rats treated with 100 mg·kg^{-1}·d^{-1} Chaga; GBM: glomerular basement membrane; FPW: foot process width; WT-1: Wilms' tumor-1. Data were presented as mean ± SD (n = 3) . $^{*}P < 0.05$ *vs* NOR; $^{\#}P < 0.05$ *vs* DN.

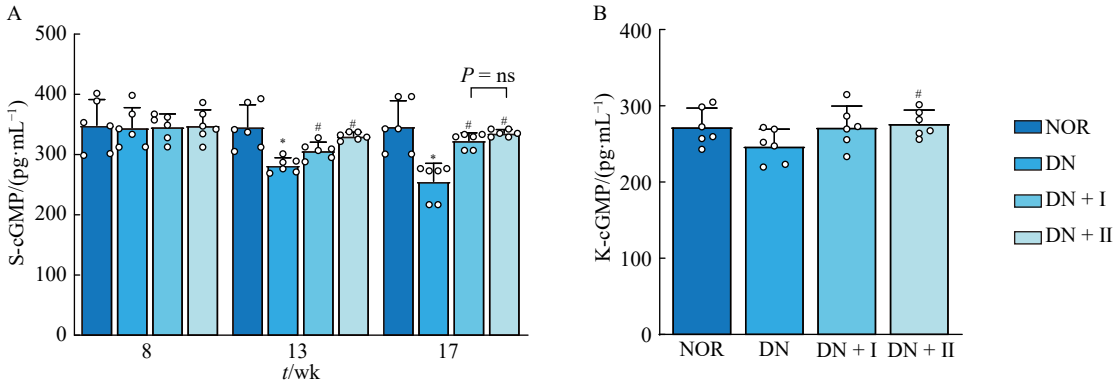

Fig. 6 Effects of Chaga on cGMP levels. (A) Levels of cGMP in serum at weeks 8, 13 and 17. (B) Levels of cGMP in kidney tissues at week 17. NOR: normal control; DN: diabetic nephropathy; DN + I: DN rats treated with 50 mg·kg^{-1}·d^{-1} Chaga; DN + II: DN rats treated with 100 mg·kg^{-1}·d^{-1} Chaga; cGMP: cyclic guanosine-3',5'-monophosphate; S-cGMP: serum cGMP; K-cGMP: kidney cGMP. Data were presented as mean ± SD (n = 6). $^{*}P < 0.05$ *vs* NOR; $^{\#}P < 0.05$ *vs* DN.

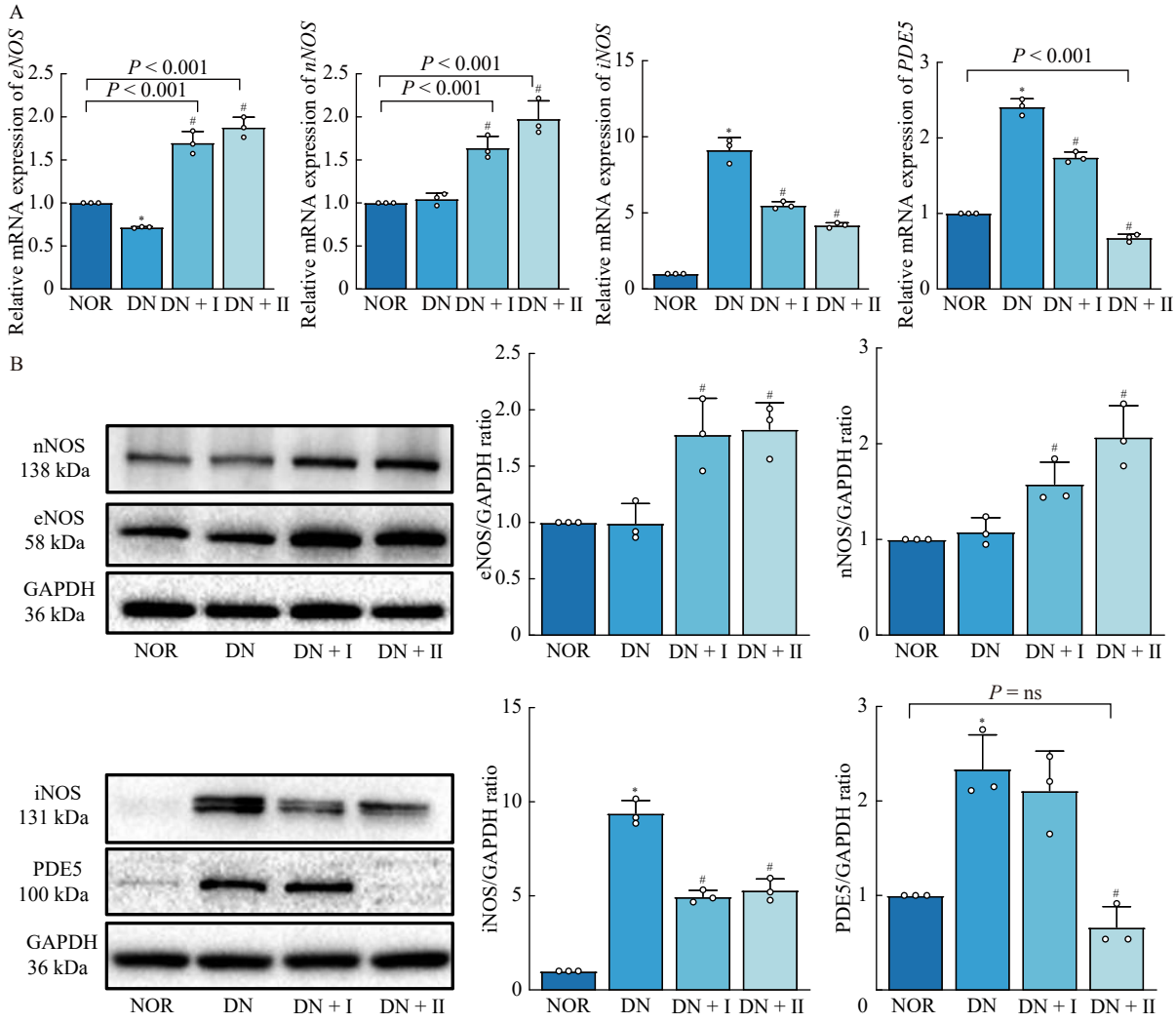

Fig. 7 Effects of Chaga on renal NOS and PDE5 expression. (A) Expression of *eNOS*, *nNOS*, *iNOS*, and *PDE5* mRNAs in kidney tissues detected by RT-PCR. (B) Expression of eNOS, nNOS, iNOS, and PDE5 proteins in kidney tissues detected by Western blot. NOR: normal control; DN: diabetic nephropathy; DN + I: DN rats treated with 50 mg·kg^{-1}·d^{-1} Chaga; DN + II: DN rats treated with 100 mg·kg^{-1}·d^{-1} Chaga; eNOS: endothelial nitric oxide synthase; nNOS: neural nitric oxide synthase; iNOS: inducible nitric oxide synthase; PDE5: phosphodiesterase 5. All data are expressed as mean ± SD (n = 3). $^{*}P < 0.05$ *vs* the NOR group; $^{\#}P < 0.05$ *vs* the DN group.

ficant value. Previous research underscores the link between kidney injury and the disruption of cGMP signaling pathway [8]. Retrospective cohort analyses have demonstrated that the beneficial effects of dapagliflozin (DAP) on SCr and CrCl levels in T2DM patients are associated with DAP's influence on gene expressions related to the cGMP signaling pathway [25]. Furthermore, *in vivo* studies on rats with cardiorenal syndrome have elucidated a direct correlation between plasma cGMP levels and the progression of renal fibrosis [26]. The decline in renal cGMP concentrations in diabetic rats has been implicated in the exacerbation of nephropathy, with treatments like cinaciguat restoring glomerular cGMP content and mitigating glomerular apoptosis and podocyte injury [27]. Building on these insights, our research posits that the beneficial effects of Chaga on improving SCr, BUN, CrCl levels, and podocyte injury may be attributed to its capacity to elevate serum cGMP levels. Moreover, the enhancement in renal cGMP levels by Chaga is likely mediated through the upregulation of renal eNOS and nNOS expression levels and the downregulation of iNOS and PDE5 expression levels. This hypothesis aligns with the observed experimental outcomes, suggesting a promising avenue for further exploration into the mechanisms underlying Chaga's renoprotective and metabolic regulatory effects.

Our prior research has demonstrated that Chaga treatment improves renal blood flow velocities, such as peak systolic velocity, end-diastolic flow velocity, and mean velocity [2]. These improvements may reflect corrections in endothelial changes brought about by the inflammatory state [28], underscoring the role of glomerular endothelial dysfunction in kidney injury progression. Notably, the *eNOS* gene is critical for controlling vascular tone [29, 30]. Our findings suggest that abnormalities in renal hemodynamic parameters in T2DM rats could be associated with the eNOS/VEGF signaling pathway [31]. Experiments on diabetic eNOS knockout (KO) mice have shown that the absence of eNOS exacerbates DN features, highlighting the potential of targeting the eNOS/cGMP pathway in preventing kidney injury [32]. Our current study further indicates that Chaga intervention initiates an increase in eNOS expression, counteracting endothelial injury and potentially preventing the reduction of eNOS expression associated with DN progression.

Nitric oxide (NO) produced by endothelial nitric oxide synthase (eNOS) and neuronal nitric oxide synthase (nNOS) predominantly engages in NO-cGMP-dependent pathways, contributing to vascular homeostasis and other physiological functions [33]. as well as iNOS-NO-non-cGMP-dependent roles in inflammatory responses, such as involvement in. In contrast, NO generated by inducible nitric oxide synthase (iNOS) can participate in both iNOS-NO-cGMP-dependent and iNOS-NO-non-cGMP-dependent pathways, the latter of which plays a significant role in inflammatory responses, including the activation of TLR-4/NF-κB signaling [34] and ERK/STAT3 pathways signaling [35]. The upregulation of iNOS is often correlated with an increase in the expression of pro-inflammatory cytokines such as TNF-α and IL-1β , leading to elevated levels of these inflammatory mediators [36]. Our study indicated that Chaga's protective effects might be attributed, in part, to its anti-inflammatory activity through the downregulation of iNOS expression. iNOS is recognized as a marker for macrophages polarized towards a pro-inflammatory phenotype in both diabetic nephropathy (DN) patient kidney biopsies and DN animal models [37]. Future research will delve into the roles of iNOS, the inflammatory response, and macrophage polarization within DN models.

The impact of Chaga on nNOS in renal health highlights an intriguing aspect of its renoprotective potential. nNOS, predominantly found in the tubular epithelium of the kidney's cortex and medulla [38], plays a vital role in renal physiology. Supplementation with naringin, for example, has been shown to restore nNOS and soluble guanylate cyclase (sGC) expression in rats with hyperammonemia, underscoring the importance of nNOS in maintaining renal function [39]. The activation of sGC by NO, produced by both eNOS and nNOS, converts guanosine triphosphate (GTP) into cGMP, a secondary messenger that is pivotal in regulating vascular tone, including that of renal arteries [40]. Renal arterial tone is largely dependent on the dilating effect of NO from eNOS and nNOS, *via* activation of sGC and cGMP action [41]. As our results suggested, Chaga may play a similar role to eNOS for nNOS.

Phosphodiesterase 5 inhibitors (PDE5is), such as sildenafil and tadalafil, enhance the physiological actions of cGMP by preventing its degradation [42]. While these inhibitors are primarily used for treating erectile dysfunction and pulmonary arterial hypertension, emerging evidence points to their beneficial effects on kidney health [12]. Studies have demonstrated the renoprotective effects of sildenafil in diabetic rats [43] and tadalafil in hypertensive nephrogenic models, suggesting a potential therapeutic pathway through the enhancement of cGMP signaling [44]. In our research, Chaga not only increased the renal expression of eNOS and nNOS but also inhibited the expression of iNOS and PDE5. This dual action likely contributes to the elevation of renal cGMP levels, mirroring the effects of PDE5.

The observed increase in serum cGMP levels suggests that Chaga's influence extends beyond the kidneys, potentially ameliorating inflammation and endothelial dysfunction systemically. Given that DN is a multifactorial disease marked by systemic inflammation, endothelial dysfunction, cardiovascular risk, and heightened clotting susceptibility, Chaga's ability to modulate circulating inflammatory molecules and promote cGMP levels presents a promising therapeutic avenue [45]. Chaga's multifaceted impact, particularly its interaction with key molecules involved in cGMP signaling, underscores its potential as a natural agent with systemic benefits.

Our study revealed a decline in serum cGMP levels during the progression to DN, indicating a direct correlation between serum cGMP levels and renal dysfunction. To illustrate, we examined CrCl as a measure of renal function, high-

lighting Chaga's potential to enhance renal function through the cGMP signaling pathway. In clinical settings, the eGFR is considered the gold standard for screening chronic kidney disease in individuals with T2DM [46]. However, due to its practicality and predictive reliability, CrCl has been utilized both clinically and in animal studies as a viable alternative to eGFR [47]. For example, the traditional herbal formula Ma-Huang Tang (MHT) was shown to reverse the decline in eNOS expression and cGMP levels in hypertensive rats, subsequently improving renal function as evidenced by CrCl [48]. This relationship between CrCl and cGMP levels was further supported by our findings following Chaga treatment.

Podocytes and their intricate foot processes are vital components of the glomerular filtration barrier, playing a key role in maintaining glomerular permeability. In a healthy state, protein kinase G (PKG) is instrumental in regulating podocyte function [49]. Research has shown that sildenafil can mitigate podocyte injury through a cGMP- and PKG-dependent mechanism, specifically by facilitating the binding of peroxisome proliferator-activated receptor γ (PPARγ) to the promoter of the transient receptor potential channel C6 [50]. This pathway underscores the therapeutic potential of targeting cGMP signaling to preserve podocyte integrity and function. In our study, we aimed to further understand the role of cGMP in influencing the expression of nephrin and WT-1, both of which are critical markers of podocyte structure. It has been observed in human podocyte models that tadalafil, a phosphodiesterase 5 inhibitor, enhances the survival of cells treated with adriamycin (ADR), an effect that is negated by inhibitors of cGMP-dependent protein kinase. This indicates that cGMP signaling through PKG plays a protective role in podocyte health. Moreover, ADR-induced reduction in the number of WT-1 positive cells, indicative of podocyte injury, can be countered by tadalafil [51]. Dysregulation of nephrin, an essential transmembrane protein in the slit diaphragm complex, is an important mechanism of foot process effacement [52].

This paper demonstrated, through *in vivo* studies, that Chaga intervention ameliorated podocyte injury. Moving forward, we plan to conduct *in vitro* experiments to not only corroborate the efficacy observed *in vivo* but also to dissect the direct impact of cGMP signaling on podocyte injury. Furthermore, the potential anti-inflammatory properties of Chaga, particularly its ability to decrease iNOS expression in T2DM rats, warrant thorough investigation. sGC and particulate guanylate cyclase (pGC) [53] are pivotal enzymes in the synthesis of cGMP synthesis. Future studies will delve deeper into the roles of sGC and pGC in cGMP synthesis, exploring additional mechanisms through which Chaga can modulate this signaling pathway and potentially offer protection against DN.

Conclusion

In summary, our research demonstrates that Chaga supplementation leads to significant improvements in glucolipid metabolism disorders and kidney injury in rats with T2DM. As illustrated in Fig. 8, the beneficial effects of Chaga on these parameters are primarily mediated through the enhancement of cGMP levels *via* multiple mechanisms: 1) activation of the eNOS/nNOS-cGMP-dependent pathway; 2) modulation of iNOS activity in a non-cGMP-dependent signaling manner; 3) inhibition of PDE5, akin to the action of PDE5 in-

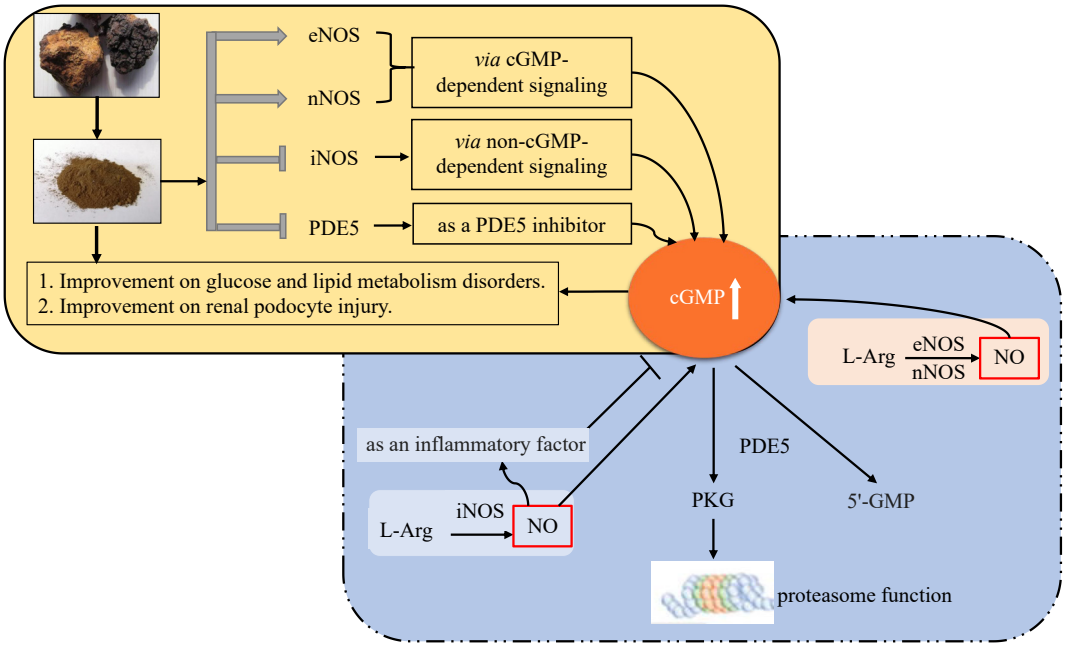

Fig. 8 The mechanism of Chaga regulating glucolipid metabolism disorders and kidney injury. eNOS: endothelial nitric oxide synthase; nNOS: neural nitric oxide synthase; iNOS: inducible nitric oxide synthase; cGMP: cyclic guanosine monophosphate; PDE5: phosphodiesterase type 5; L-Arg: L-arginine; NO: nitric oxide; PKG: activates protein kinase G.

hibitors. This multifaceted approach enables Chaga to not only rectify glucolipid metabolism disturbances observed during the T2DM stage but also ameliorate renal damage characteristic of the DN stage. These effects are intricately linked to the cGMP signaling pathway, with eNOS, nNOS, and PDE5 playing distinct roles in modulating this pathway. Specifically, Chaga augments eNOS and nNOS levels to promote beneficial renal physiological effects *via* a cGMP-dependent route, diminishes iNOS levels to attenuate pro-inflammatory responses, and curtails cGMP hydrolysis through PDE5 inhibition. The findings from this study furnish compelling evidence supporting the potential application of Chaga in the clinical prevention and treatment of DN. They also shed light on the underlying mechanisms by which Chaga exerts its renoprotective and metabolic regulatory effects.

References

[1] Kou RW, Han R, Gao YQ, *et al*. Anti-neuroinflammatory polyoxygenated lanostanoids from Chaga mushroom *Inonotus obliquus* [J]. *Phytochemistry*, 2021, **184**: 112647.

[2] Zhang Z, Liang X, Tong L, *et al*. Effect of *Inonotus obliquus* (Fr.) Pilat extract on the regulation of glycolipid metabolism *via* PI3K/Akt and AMPK/ACC pathways in mice [J]. *J Ethnopharmacol*, 2021, **273**: 113963.

[3] Zhang Y, Liao H, Shen D, *et al*. Renal protective effects of *Inonotus obliquus* on high-fat diet/streptozotocin-induced diabetic kidney disease rats: biochemical, color doppler ultrasound and histopathological evidence [J]. *Front Pharmacol*, 2022, **12**: 743931.

[4] Sohrabi M, Binaeizadeh MR, Iraji A, *et al*. A review on *α*-glucosidase inhibitory activity of first row transition metal complexes: a futuristic strategy for treatment of type 2 diabetes [J]. *RSC Adv*, 2022, **12**(19): 12011-12052.

[5] Wong YH, Wong SH, Wong XT, *et al*. Genetic associated complications of type 2 diabetes mellitus [J]. *Panminerva Med*, 2022, **64**(2): 274-288.

[6] Hua Q, Han Y, Zhao H, *et al*. Punicalagin alleviates renal injury *via* the gut-kidney axis in high-fat diet-induced diabetic mice [J]. *Food Funct*, 2022, **13**(2): 867-879.

[7] Teh YM, Mualif SA, Lim SK. A comprehensive insight into autophagy and its potential signaling pathways as a therapeutic target in podocyte injury [J]. *Int J Biochem Cell Biol*, 2022, **143**: 106153.

[8] Hu L, Chen Y, Zhou X, *et al*. Effects of soluble guanylate cyclase stimulator on renal function in ZSF-1 model of diabetic nephropathy [J]. *PLoS One*, 2022, **17**(1): e0261000.

[9] Rogacka D, Rachubik P, Audzeyenka I, *et al*. Enhancement of cGMP-dependent pathway activity ameliorates hyperglycemia-induced decrease in SIRT1-AMPK activity in podocytes: impact on glucose uptake and podocyte function [J]. *Biochim Biophys Acta Mol Cell Res*, 2022, **1869**(12): 119362.

[10] Ma L, Hu L, Jin L, *et al*. Rebalancing glucolipid metabolism and gut microbiome dysbiosis by nitrate-dependent alleviation of high-fat diet-induced obesity [J]. *BMJ Open Diabetes Res Care*, 2020, **8**(1): e001255.

[11] Liao H, Jia D, Zhao X, *et al*. Effects of Chaga medicinal mushroom *Inonotus obliquus* (Agaricomycetes) extracts on NOS-cGMP-PDE5 pathway in rat penile smooth muscle cells [J]. *Int J Med Mushrooms*, 2020, **22**(10): 979-990.

[12] Coskuner ER, Ozkan B. Reno-protective effects of phosphodiesterase 5 inhibitors [J]. *Clin Exp Nephrol*, 2021, **25**(6): 585-597.

[13] Fanali C, Gallo V, Della PS, *et al*. Choline chloride-lactic acid-based NADES as an extraction medium in a response surface methodology-optimized method for the extraction of phenolic compounds from hazelnut skin [J]. *Molecules*, 2021, **26**(9): 2652.

[14] Li W, Jiang L, Lu X, *et al*. Curcumin protects radiation-induced liver damage in rats through the NF-*κ*B signaling pathway [J]. *BMC Complement Med Ther*, 2021, **21**(1): 10.

[15] Zhang KQ, Tian T, Hu LL, *et al*. Effect of probucol on autophagy and apoptosis in the penile tissue of streptozotocin-induced diabetic rats [J]. *Asian J Androl*, 2020, **22**(4): 409-413.

[16] Wilson RD, Islam MS. Fructose-fed streptozotocin-injected rat: an alternative model for type 2 diabetes [J]. *Pharmacol Rep*, 2012, **64**(1): 129-139.

[17] Liu JY, Mu S, Zhang SP, *et al*. Roux-en-Y gastric bypass surgery suppresses hypothalamic PTP1B protein level and alleviates leptin resistance in obese rats [J]. *Exp Ther Med*, 2017, **14**(3): 2536-2542.

[18] Xu LL, Gao W, Chen ZM, *et al*. Relationships between diabetic nephropathy and insulin resistance, inflammation, Trx, Txnip, CysC and serum complement levels [J]. *Eur Rev Med Pharmacol Sci*, 2020, **24**(22): 11700-11706.

[19] Zeng JY, Wang Y, Miao M, *et al*. The effects of rhubarb for the treatment of diabetic nephropathy in animals: a systematic review and meta-analysis [J]. *Front Pharmacol*, 2021, **12**: 602816.

[20] Wang C, Liang J, Yang W, *et al*. Ultra-performance liquid chromatography-Q-exactive orbitrap-mass spectrometry analysis for metabolic communication between heart and kidney in adriamycin-induced nephropathy rats [J]. *Kidney Blood Press Res*, 2022, **47**(1): 31-42.

[21] Wang C, Hou XX, Rui HL, *et al*. Artificially cultivated *Ophiocordyceps sinensis* alleviates diabetic nephropathy and its podocyte injury *via* inhibiting P2X7R expression and NLRP3 inflammasome activation [J]. *J Diabetes Res*, 2018, **2018**: 1390418.

[22] Everaert I, Van der ST, Stautemas J, *et al*. Oral anserine supplementation does not attenuate type-2 diabetes or diabetic nephropathy in BTBR ob/ob mice [J]. *Amino Acids*, 2021, **53**(8): 1269-1277.

[23] Li Y, Gong W, Liu J, *et al*. Angiopoietin-like protein 4 promotes hyperlipidemia-induced renal injury by down-regulating the expression of ACTN4 [J]. *Biochem Biophys Res Commun*, 2022, **595**: 69-75.

[24] Ladeira LCM, Dos Santos EC, Santos TA, *et al*. Green tea infusion prevents diabetic nephropathy aggravation in recent-onset type 1 diabetes regardless of glycemic control [J]. *J Ethnopharmacol*, 2021, **274**: 114032.

[25] Chen G, Wang H, Zhang W, *et al*. Dapagliflozin reduces urinary albumin excretion by downregulating the expression of cAMP, MAPK, and cGMP-PKG signaling pathways associated genes [J]. *Genet Test Mol Biomarkers*, 2021, **25**(10): 627-637.

[26] Qiu Q, Cao J, Wang Y, *et al*. Time course of the effects of Buxin Yishen Decoction in promoting heart function and inhibiting the progression of renal fibrosis in myocardial infarction caused type 2 cardiorenal syndrome rats [J]. *Front Pharmacol*, 2019, **10**: 1267.

[27] Czirok S, Fang L, Radovits T, *et al*. Cinaciguat ameliorates glomerular damage by reducing ERK1/2 activity and TGF-β expression in type-1 diabetic rats [J]. *Sci Rep*, 2017, **7**(1): 11218.

[28] Chekalina NI, Burmak YH, Petrov YY, *et al*. Justification of increasing the blood flow velocity in the arteries of the thyroid

gland in autoimmune thyroiditis as a reflection of endothelial changes due to inflammatory status [J]. *Curr Med Imaging Rev*, 2019, **15**(1): 61-65.
[29] Fu Y, Wang X, Zhang L, *et al*. Allograft inflammatory factor-1 enhances inflammation and oxidative stress *via* the NF-κB pathway in diabetic kidney disease [J]. *Biochem Biophys Res Commun*, 2022, **614**: 63-69.
[30] Xie X, Shi X, Xun X, *et al*. Endothelial nitric oxide synthase gene single nucleotide polymorphisms and the risk of hypertension: a meta-analysis involving 63 258 subjects [J]. *Clin Exp Hypertens*, 2017, **39**(2): 175-182.
[31] Wang J, Feng Y, Zhang Y, *et al*. TNF-α and IL-1β promote renal podocyte injury in T2DM rats by decreasing glomerular VEGF/eNOS expression levels and altering hemodynamic parameters [J]. *J Inflamm Res*, 2022, **15**: 6657-6673.
[32] Harloff M, Prüschenk S, Seifert R, *et al*. Activation of soluble guanylyl cyclase signalling with cinaciguat improves impaired kidney function in diabetic mice [J]. *Br J Pharmacol*, 2022, **179**(11): 2460-2475.
[33] Ferrini MG, Garcia E, Abraham A, *et al*. Effect of ginger, *Paullinia cupana*, *Muira puama* and L-citrulline, singly or in combination, on modulation of the inducible nitric oxide-NO-cGMP pathway in rat penile smooth muscle cells [J]. *Nitric Oxide*, 2018, **76**: 81-86.
[34] Abdel-Hakeem EA, Abdel Hafez SMN, Kamel BA, *et al*. Angiotensin 1−7 mitigates rhabdomyolysis induced renal injury in rats *via* modulation of TLR-4/NF-κB/iNOS and Nrf-2/heme-oxygenase-1 signaling pathways [J]. *Life Sci*, 2022, **303**: 120678.
[35] Wu JY, Xie JH, Chen YJ, *et al*. Amelioration of TPA-induced skin inflammation by the leaf extract of *Vernonia amygdalina* involves ERK/STAT3 (Ser727) signaling inhibition [J]. *Phytomedicine*, 2022, **102**: 154194.
[36] Assar DH, Asa SA, El-Abasy MA, *et al*. *Aspergillus awamori* attenuates ochratoxin A-induced renal and cardiac injuries in rabbits by activating the Nrf2/HO-1 signaling pathway and downregulating IL1β, TNFα, and iNOS gene expressions [J]. *Environ Sci Pollut Res Int*, 2022, **29**(46): 69798-69817.
[37] Ma T, Li X, Zhu Y, *et al*. Excessive activation of Notch signaling in macrophages promote kidney inflammation, fibrosis, and necroptosis [J]. *Front Immunol*, 2022, **13**: 835879.
[38] Slyvka Y, Malgor R, Inman SR, *et al*. Antioxidant diet and sex interact to regulate NOS isoform expression and glomerular mesangium proliferation in Zucker diabetic rat kidney [J]. *Acta Histochem*, 2016, **118**(2): 183-193.
[39] Xiao S, Li Q, Hu L, *et al*. Soluble guanylate cyclase stimulators and activators: where are we and where to go [J]. *Mini Rev Med Chem*, 2019, **19**(18): 1544-1557.
[40] Giandalia A, Alibrandi A, Giorgianni L, *et al*. Resistin levels and inflammatory and endothelial dysfunction markers in obese postmenopausal women with type 2 diabetes mellitus [J]. *Diabetol Metab Syndr*, 2021, **13**(1): 98.
[41] Wennysia IC, Zhao L, Schomber T, *et al*. Role of soluble guanylyl cyclase in renal afferent and efferent arterioles [J]. *Am J Physiol Renal Physiol*, 2021, **320**(2): F193-F202.
[42] Tzoumas N, Farrah TE, Dhaun N, *et al*. Established and emerging therapeutic uses of PDE type 5 inhibitors in cardiovascular disease [J]. *Br J Pharmacol*, 2020, **177**(24): 5467-5488.
[43] Mehanna OM, El-Askary A, Al-Shehri S, *et al*. Effect of phosphodiesterase inhibitors on renal functions and oxidant/antioxidant parameters in streptozocin-induced diabetic rats [J]. *Arch Physiol Biochem*, 2018, **124**(5): 424-429.
[44] Tomita N, Hotta Y, Naiki-Ito A, *et al*. The phosphodiesterase 5 inhibitor tadalafil has renoprotective effects in a rat model of chronic kidney disease [J]. *Physiol Rep*, 2020, **8**(17): e14556.
[45] Pretorius E. Platelets as potent signaling entities in type 2 diabetes mellitus [J]. *Trends Endocrinol Metab*, 2019, **30**(8): 532-545.
[46] Mao F, Liu S, Qiao X, *et al*. SUDOSCAN, an effective tool for screening chronic kidney disease in patients with type 2 diabetes [J]. *Exp Ther Med*, 2017, **14**(2): 1343-1350.
[47] Schini M, Peel N, Toronjo-Urquiza L, *et al*. Evaluation of estimated glomerular function (eGFR) versus creatinine clearance (CrCl) to predict acute kidney injury when using zoledronate for the treatment of osteoporosis [J]. *Osteoporos Int*, 2022, **33**(3): 737-744.
[48] Hong MH, Kim HY, Jang YJ, *et al*. New therapeutic insight into the effect of Ma Huang Tang on blood pressure and renal dysfunction in the L-NAME-induced hypertension [J]. *Evid-Based Compl Alt*, 2021, **2021**: 9980429.
[49] Piwkowska A. Role of protein kinase G and reactive oxygen species in the regulation of podocyte function in health and disease [J]. *J Cell Physiol*, 2017, **232**(4): 691-697.
[50] Sonneveld R, Hoenderop JG, Isidori AM, *et al*. Sildenafil prevents podocyte injury *via* PPAR-γ-mediated TRPC6 inhibition [J]. *J Am Soc Nephrol*, 2017, **28**(5): 1491-1505.
[51] Tomita N, Hotta Y, Naiki-Ito A, *et al*. Protective effects of tadalafil on damaged podocytes in an adriamycin-induced nephrotic syndrome model [J]. *J Pharmacol Sci*, 2022, **149**(2): 53-59.
[52] Nakamichi R, Hayashi K, Itoh H. Effects of high glucose and lipotoxicity on diabetic podocytes [J]. *Nutrients*, 2021, **13**(1): 241.
[53] Chen Y, Burnett JC. Particulate guanylyl cyclase A/cGMP signaling pathway in the kidney: physiologic and therapeutic indications [J]. *Int J Mol Sci*, 2018, **19**(4): 1006.

Cite this article as: FENG Yating, LIU Jing, GONG Le, *et al*. *Inonotus obliquus* (Chaga) against HFD/STZ-induced glucolipid metabolism disorders and abnormal renal functions by regulating NOS-cGMP-PDE5 signaling pathway [J]. *Chin J Nat Med*, 2024, **22**(7): 619-631.